

**Combustion characteristics of blends of kerosene and
cooking oil at various fuel-air equivalence ratio:
Simulation approach**

MOHAMMAD 'ASRI BIN KADIR

UNIVERSITI SAINS MALAYSIA

2021

Combustion characteristics of blends of kerosene and cooking oil at various fuel-air equivalence ratio: Simulation approach

By:

MOHAMMAD ‘ASRI BIN KADIR

(Matrix no.: 137830)

Supervisor:

DR. KHAIRIL FAIZI MUSTAFA

July 2021

This dissertation is submitted to

Universiti Sains Malaysia

As partial fulfillment of the requirement to graduate with honors degree in

BACHELOR OF ENGINEERING (MECHANICAL ENGINEERING)



School of Mechanical Engineering
Engineering Campus
Universiti Sains Malaysia

DECLARATION


This work has not previously been accepted in substance for any degree and is not being concurrently submitted in candidature for any degree.

Signed..........(Mohammad 'Asri Bin Kadir)

Date..11 July 2021.....

Statement 1

This journal paper is the result of my own investigation, except where otherwise stated. Other sources are acknowledged by giving explicit references. Bibliography/references are appended.

Signed..........(Mohammad 'Asri Bin Kadir)

Date..11 July 2021.....

Statement 2

I hereby give consent for my journal paper, if accepted, to be available for photocopying and for interlibrary loan, and for the title and summary to be made available outside organizations.

Signed..........(Mohammad 'Asri Bin Kadir)

Date..11 July 2021.....

ACKNOWLEDGEMENT



In the name of Allah, the Most Gracious and the Most Merciful. Praise to Allah the almighty god who has given me strength physically and mentally, time and guidance throughout my journey in finishing my final year project report.

I would like to express my deepest thank you to my supervisor, Dr. Khairil Faizi Mustafa for the guidance and support throughout my final year in conducting and writing the final year project report.

Also not forget Dr. Muhammad Fauzinizam Razali, the coordinator of this final year project that has help in organizing seminar with useful information that helped me to write a better report.

Last but not least, my friends and family who always encouraged and motivate me in doing my research. I am also very thankful for each individual for their direct and indirect involvement throughout this project.

TABLE OF CONTENTS

ACKNOWLEDGEMENT	iv
TABLE OF CONTENTS	v
LIST OF FIGURES	vii
LIST OF ABBREVIATIONS	viii
ABSTRAK	ix
ABSTRACT	x
CHAPTER 1 INTRODUCTION	1
1.1 Introduction	1
1.2 Project Background	4
1.3 Problem Statement	5
CHAPTER 2 LITERATURE REVIEW	7
2.1 Kerosene and vegetable oil blend.....	7
2.2 Thermoelectric generators (TEGs).....	8
2.3 Temperature difference of thermoelectric generator	10
2.4 The effect of internal and external resistance.....	12
CHAPTER 3 RESEARCH METHODOLOGY	14
3.1 Combustion modelling for hot side of TEG.....	15
3.2 The cold side of TEG	17
3.3 The power generated by TEG	20
CHAPTER 4 RESULTS AND DISCUSSION	21
4.1 Combustion modelling for hot side of TEG.....	21
4.2 The cold side of TEG	24
4.3 The power generated by TEG	28

CHAPTER 5 CONCLUSION AND FUTURE WORK	31
REFERENCES.....	32
APPENDICES	

LIST OF FIGURES

	Page
Figure 1.1 Thermoelectric cell	2
Figure 1.2 Heat transfer in the TEGs	4
Figure 2.1 Components in thermoelectric generator.....	8
Figure 3.1 TEG module.....	Error! Bookmark not defined.
Figure 3.2 Combustion Chamber	15
Figure 3.3 TEG with water heat exchanger	19
Figure 4.1 Temperature distribution of the wall	22
Figure 4.2 Temperature distribution along x-axis at $y=0.075\text{m}$ and $y=0.22\text{m}$	22
Figure 4.3 Wall Temperature Vs Fuel Blend at different Φ	23
Figure 4.4 Wall Temperature Vs Fuel Blend at Different Φ with fix air flow rate ...	23
Figure 4.5 Temperature distribution on the TEG with water heat exchanger.....	25
Figure 4.6 Temperature different vs fuel blend at $\Phi=1$ with different water flow rate.....	25
Figure 4.7 Temperature different vs fuel blend at $\Phi=0.75$ with different water flow rate	26
Figure 4.8 Temperature different vs fuel blend at $\Phi=0.3$ with different water flow rate	26
Figure 4.9 Temperature different of 100%Kerosene at different Φ vs water flow rate.....	27
Figure 4.10 Voltage vs current.....	29
Figure 4.11 Power vs fuel blend with $\Phi=0.3$ for different water flow rate	29
Figure 4.12 Power vs fuel blend with $\Phi=0.75$ for different water flow rate	30
Figure 4.13 Power vs fuel blend with $\Phi=1.0$ for different water flow rate	30

LIST OF ABBREVIATIONS

AHS	Aluminum Heat Sink
GTEG	Geothermal Thermoelectric Generator
KVCO	Kerosene-Vegetable Cooking Oil Blend
LHV	Low Heating Value
PEMFC	Proton Exchange Membrane Fuel Cell
RCHS	Radiative Cooling Heat Sink
TEG	Thermoelectric Generator
A	Ampere
ρ	Density
Φ	Equivalent air fuel ratio
Cp	Specific heat capacity
k	Thermal conductivity
V	Volt

ABSTRAK

Satu simulasi telah dijalankan bagi menilai prestasi penjana termoelektrik, dengan bantuan penukar haba cecair menggunakan air. Simulasi ini terbahagi kepada tiga bahagian iaitu model pembakaran kerosin-minyak masak sayuran, KVCO untuk bahagian panas penjana termoelektrik, suhu di bahagian sejuk penjana termoelektrik menggunakan penukar haba cecair dan kuasa yang dapat dijana oleh TEG. Dalam kajian ini, TEG terdiri daripada 128 jenis-p dan 128 jenis-n semikonduktor PbTe. Model bagi pembakaran KVCO menggunakan 5 campuran berbeza iaitu 100% Kerosin, 90% Kerosin, 75% Kerosin, 50% Kerosin dan juga 25% Kerosin. Selain itu, tiga kadar pengaliran air ke dalam penukar haba cecair yang berbeza, 0.005kg/s, 0.01kg/s dan 0.03kg/s digunakan bagi menjalankan simulasi untuk mendapatkan suhu di bahagian sejuk TEG. Kuasa maksimum yang dapat direkod dari simulasi menunjukkan nilai sebanyak 227mW pada tetapan 100% Kerosin dan 0.03 kg/s kadar aliran air. Selain itu, nilai perbezaan potensi dari 0.12 V ke 0.19 V serta nilai arus dari 0.5 A ke 1.2 A telah direkod daripada simulasi ini.

ABSTRACT

A simulation has been conducted to evaluate the performance of a thermoelectric generator, with water-cooled heat exchanger. The simulation was conducted for three parts, which were the combustion of kerosene-vegetable cooking oil blend model, the temperature of cold side of TEG with water-cooled heat exchanger and the power generated by TEG. The plumbum telluride thermoelectrics module consists of 128 p-type and 128 n-type semiconductor legs. The model for combustion was conducted using five different blends of kerosene-vegetable cooking oil which were 100% Kerosene, 90% Kerosene, 75% Kerosene, 50% Kerosene and 25% Kerosene. Three different water flow rates of 0.005kg/s, 0.01kg/s and 0.03kg/s flow into the heat exchanger to simulate the temperature at the cold side of the thermoelectric generator. A maximum power output of 227 mW was achieved using 100% kerosene at 0.03 kg/s. The potential difference ranged between 0.12V to 0.19V and the current ranged between 0.5A – 1.2 A.

CHAPTER 1

INTRODUCTION

1.1 Introduction

Thermoelectricity is the conversion of thermal energy into electrical energy or vice versa. Based on the Seebeck effect, the temperature difference is the primary driving force for the generation of electricity. Despite a relatively low thermal efficiency (approximately 5% - 8%), thermoelectric devices are capable of operating quietly and zero carbon footprint, and it gives promising alternatives for sustainability and environmentally friendly in the energy generation. Many research works have been conducted on heat recovery using the thermoelectric generators to increase the efficiency of the system[1][2][3].

By taking the advantage of Seebeck effect, the thermoelectric generators (TEGs) convert the heat energy into electricity. The temperature gradient influences the output performance of the TEGs, where the higher the temperature gradient, the higher the power that can generated. In order to increase the temperature gradient, a heat exchanger is usually being used at both the cold and hot sides of the TEGs.

One thermoelectric cell consists of two different thermoelectric materials and metal conductors.

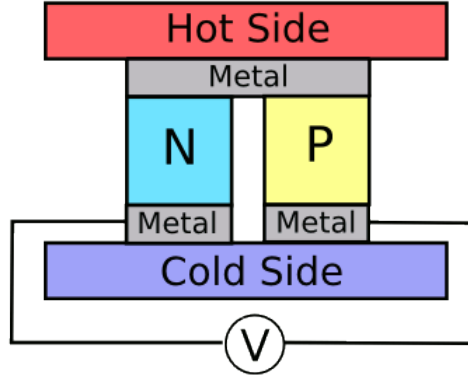


Figure 1-1 Thermoelectric cell

The voltage generated from TEGs can be expressed as[4]

$$V_{out} = N\alpha_{AB}\Delta T \quad 1.1$$

Where N is the number of connected thermocouples, α_{AB} is the Seebeck coefficient of the connected thermocouple ($\alpha_{AB} = \alpha_A - \alpha_B$) and ΔT is the temperature gradient between the hot and cold sides of the thermocouples. The internal resistance of TEGs that is electrically connected in series is proportional to the number of N. Therefore, by increasing the number of thermocouples the voltage generated can be increased and it impacts in increasing of the internal resistance of TEG. The internal resistance of TEGs can be expressed as [5]

$$R_{TEG} = N\left(\frac{\rho}{A} + 2\frac{\rho_C L_C}{A_C}\right) \quad 1.2$$

Where ρ is the resistivity of the thermocouples, ρ_C is the contact metal resistivity, A is the thermocouple cross-sectional area and A_C is the contact metal cross sectional area. The output power generated from TEGs can be expressed as

$$P_{out} = V_{out}^2 \left(\frac{R_L}{R_{TEG} + R_L} \right)^2 \quad 1.3$$

R_L is the load resistances. The maximum load can be achieved when load resistance equal to internal resistance of TEGs.

$$P_{max} = \left(\frac{V_{out}^2}{R_{TEG}^2} \right) \quad 1.4$$

1.2 Project Background

Thermoelectricity has spark interest from many researchers due to its compactness and quiet operation as there are no moving parts. There are a lot of thermoelectric materials that are available currently such as Bismuth Telluride (Bi_2Te_3) and Lead Telluride (PbTe). The efficiency of the material can be indicated by figure-of-merit (zT). However, the main focus of this project is the performance of TEGs with the presence of heat exchanger in order to enhance the heat flow in the system. By using heat exchangers, the temperature gradient between the hot and cold side of TEGs can be increased. From equation (1) we can observe that the output voltage depends on the temperature gradient.

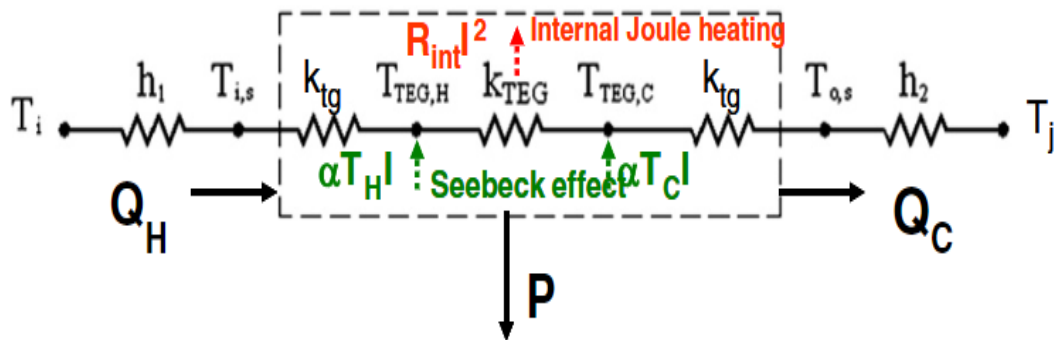


Figure 1-2 Heat transfer in the TEGs

In Figure 1-2, heat from the surrounding air with T_i is transferred to the metal plate with heat transfer coefficient of h_1 . The heat then flows across the TEGs with thermal conductivity of k_{TEG} from the hot side with the temperature of T_H to the cold side with the temperature of T_C . Heat is transferred to the water inside the heat exchanger through forced convection. From this, we can see that the power generated is simply the different between Q_H and Q_C [6].

$$P = Q_H - Q_C \quad 1.5$$

Where,

$$Q_H = N\alpha T_H I - \frac{1}{2} I^2 R_{TEG} + Nk_{TEG}(T_H - T_C) \quad 1.6$$

And

$$Q_C = N\alpha T_C I + \frac{1}{2} I^2 R_{TEG} + Nk_{TEG}(T_H - T_C) \quad 1.7$$

Therefore,

$$P = N\alpha I(T_H - T_C) - I^2 R_{TEG} \quad 1.8$$

Where k_{TEG} is the thermal conductivity of TEGs.

1.3 Problem Statement

Heat waste is one of the challenges in many industrial applications. Heat energy which is produce from a system such as combustion in car engine or electric generator engine needs to be managed to reduce the heat waste as well as increasing the overall efficiency of the system. Therefore, by implementing heat waste recovery system, the efficiency of a system can be increased.

1.4 Objectives

The objectives of this study are to;

- i. To simulate the temperature distribution by the combustion of kerosene-vegetable cooking oil.
- ii. To simulate the power generated by the thermoelectric generator.

CHAPTER 2

LITERATURE REVIEW

This review will be focusing on the output performance such as current, voltage and power generated by the TEGs that use the combustion of kerosene and vegetable oil blend as the heat source. Numerous studies have been conducted to evaluate the output performance of the TEGs under various input parameters such as the temperature, arrangement between the TEGs and type of TEGs.

2.1 Kerosene and vegetable oil blend

In order to model the combustion of the kerosene and oil blends, it is very important to determine the lower heating value (LHV) of both fuels. Generally, the LHV of kerosene is approximately 43.1 MJ/kg and this value depends on its chemical composition and impurities [7]. Ameer Uddin et al. [8] suggested that the LHV of 100% kerosene is 44.8 MJ/kg. The LHV varies from 35.96 MJ/kg (50% kerosene and 50% pure mustard oil blend) to 42.8 KJ/kg (80% kerosene and 20% pure mustard oil blend). In addition, the paper also suggested that the LHV of pure mustard oil is 32.43 MJ/kg.

Another research work was conducted by Bayındır et al. to investigate the performance of the diesel power generator fuelled by biodiesel-kerosene and biodiesel-kerosene-diesel blends [9]. The research found that the LHV of kerosene and neat safflower oil is 43.5 MJ/kg and 39.66 MJ/kg, respectively. Furthermore, 20% kerosene and 80% neat safflower oil yields an LHV of 41.007MJ/kg.

2.2 Thermoelectric generators (TEGs)

Thermoelectric generators usually consist of many pairs of n-type and p-type semiconductor connected electrically in series as shown in Figure 2-1. Ceramic plate is attached at both end of the legs in order to create higher temperature different between the hot and cold side for maximum power generation. The most common thermoelectric materials are Bismuth Telluride (Bi_2Te_3), Lead Telluride (PbTe) and Silicon Germanium (SiGe). Figure of merit (zT) shows the degree of capability of the materials to generate thermoelectric power.

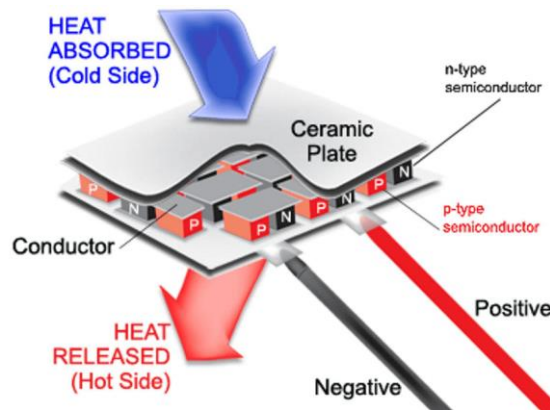


Figure 2-1 Components in thermoelectric generator

Many research has been conducted to discover new thermoelectric materials. A research has done by Bu et al. on the rhombohedral $\text{Ge}_{1-x}\text{Pb}_x\text{Te}$ thermoelectric [10]. The material is prepared by ice-water-quenched from high temperature single phase region. The study obtained an average zT value of 0.7 at the temperature of 200K-350K using $\text{Ge}_{0.42}\text{Pb}_{0.58}\text{Te}$. The writer emphasized that $\text{Ge}_{1-x}\text{Pb}_x\text{Te}$ solid solution can be a highly competition thermoelectric figure of merit to the conventional p- Bi_2Te_3 alloys at near room temperature.

Another thermoelectric material is $(\text{GeTe})_{100-x}(\text{AgSbTe}_2)_x$ also known as TAGS (Te/Ag/Ge/Sb) are use in mid-temperature range applications due to good electrical and thermal properties (Zybała et al., 2020). However, TAGS has very low

Seebeck coefficient and a study is conducted by Zybala et al. to optimize TAGS by introducing $AgSbSe_2$ as doping to the structure. Composition of $(GeTe)_{75}(AgSbTe_2)_x(AgSbSe_2)_y$ is synthesized with value of $y = (0, 0.26, 0.51, 1.25$ and $6.25)$ where $x + y = 25$. Doped TAGS with addition $AgSbSe_2$ ($y=1.25$) resulted in an increase of Seebeck coefficient from 50 to 100 $\mu V/K$ and the maximum zT of 1.2 is recorded at temperature of 323-625 K.

A research on sodium doped cobalt oxide Na_xCoO_2 is done by Akram et al. to enhance the properties of thermoelectric material [12]. Different value of x is used which is 1, 0.98, 0.96 and 0.94. The writer suggests that as the concentration of Na is decreasing, the thermal and electrical conductivity is enhanced as well as Seebeck coefficient. A value of 1.24 zT is achieved at 1010K that give an increasing of 28% from un-doped materials.

In addition, Mo et al. has conducted a study on the performance on n-type Mg_3Bi_2 with Se doping at room temperature where maximum value of zT of 1.24 is obtained at temperature of 498K using $Mg_{3.2}Bi_{1.4}Sb_{0.59}Se_{0.1}$ and minimum zT value of 0.82 at temperature of 300K.

Thermoelectric generator is electrical component that produce electricity based on the temperature different on the hot and cold side of TEGs. Many studies have been conducted to investigate as well as optimizing the performance of TEGs.

2.3 Temperature difference of thermoelectric generator

TEGs principally operate due to the temperature difference, and the TEGs are always seen to be a good candidate to be used in heat waste recovery. One of the studies that has been conducted on TEGs used exhaust gas from vehicles as the heat source [2]. A simulation is used to model the output power and efficiency under various factors such as exhaust flow rate, flow rates of different cooling fluid, heat convection coefficient, the height of P-N couple and the ratio between the external resistance to the internal resistance of the circuit. From the simulation, the power output and efficiency increase nonlinearly with an increase in the mass flow rate of the cooling fluid. The power output and the efficiency increase at a lower rate as the mass flow rate increases beyond 40g/s. Then, an increase in the power output of 20W was obtained when the mass flow rate of an exhaust gas was increased from 10g/s to 30 g/s. This increase was considered very low. An increase in the heat convection coefficient will also result in an increase in the power output and efficiency. Another parameter is the height, H on the PN couple. An increase in the height will also result in an increase in the output power and efficiency. However, a further increase in the height also increases the internal resistance thus reducing the power output. Another important variable is the effect of ratio between the external to internal resistance where the maximum output power was found to 1.5.

Another study was done on waste heat recovery of Proton Exchange Membrane Fuel Cell (PEMFC) where the performance characteristics was measured at different conditions of natural and forced convection [14]. The hot side of the TEG was attached to PEMFC while the cold side of TEG was attached to metal hydride (MH) cylinder. The maximum temperature difference between the hot and cold sides of 3.2 °C was obtained with the maximum power output of 27 mW.

In addition, a study on the effects of axial conduction on the performance of thermoelectric generators integrated in a heat exchanger for waste recovery application was carried out [15]. In the study, a numerical model was created whereby two to eight TEGs were used with the flow rate of exhaust gas ranged between 0.02 kg/s to 0.08 kg/s. Furthermore, an experimental set up was developed to validate the numerical model. Power gain, which is the ratio between the power output from a system without an axial conduction to the power output from a system with axial conduction was introduced in the study. A power gain of 1.2 which is equivalent to 20% increase in the power output was obtained at low exhaust flow rate of 0.02kg/s. The maximum power output of 170 W was also obtained at 0.08kg/s exhaust flow rate using six rows of TEGs.

A study was performed to investigate the effect of cooling performance on the cold side to the output performance of TEGs. A study of radiative cooling on the cold side of TEGs which affected the output performance was conducted by Liu et al. [16]. In their study, a model was created using TEGs with radiative cooling heat sink (TEG-RCHS) . During the operation, TEG-RCHS module generated a total power of about 32% higher compared with the TEGs with an aluminum heat sink (TEG-AHS). However, the results indicate that the wind speed and the heater temperature yield positive effects while the ambient humidity and temperature adversely affected the power generation. The experiment was conducted in two places which were at an arid area and at a humid area. At the arid area, the sky is clear with solar radiation around 950 W/m², the humidity recorded was between 25% to 75% and the wind velocity recorded was between 0 to 2 m/s. In this area, a temperature difference of 3.25 K and 2.62 K were achieved by TEG-RCHS and TEG-AHS respectively. This temperature difference yields a total energy generation

of 54.8 Wh/m² and 41.2 Wh/m² by TEG-RCHS and TEG-AHS, respectively. In the humid area, the sky was overcast with 980 W/m² radiation and occasionally reduced to 350 W/ m². The relative humidity fell between 60% and 98% with the wind speed between 0 m/s to 1 m/s. In humid area the temperature difference of 3.35K and 3.16 K is recorded from TEG-RCHS and TEG-AHS respectively. This yield energy generation of 54.1 Wh/m² and 51.5 Wh/m² by TEG-RCHS and TEG-AHS respectively. Another study was conducted in the shallow hot dry rock fields [17]. The objective of this experimental work was to investigate the power generation of Geothermal Thermoelectric Generator (GTEG). There were two types of cold side heat exchanger which were the fin dissipators assisted by fan and loop thermosyphons. For the cold side heat exchanger, 150 mm and 250 mm long fin dissipators were used while eight and six condensation level loops thermosyphon were used. The results suggested that the loop thermosyphons were found to be a better option where the power generated of up to 3.3 W and 2.4 W were generated when eight and six level loop thermosyphons were used.

2.4 The effect of internal and external resistance

Another parameter that influences the performance of the TEGs is the internal resistance of the TEGs and the external resistance of the load. Attar et al. suggested that there is optimum load resistance that should be used in order to get the maximum power output generated by the TEGs [6]. In their study, the optimum load resistance was obtained by an analytical method using a dimensional analysis. The ratio between the internal resistance and the external resistance (R_r) of the load was introduced to create a dimensionless parameter. From the analysis, the maximum

power was obtained when the internal resistance is equal to the external resistance. The maximum power of 0.065 W was recorded when $R_r=1$. However, Attar et al. [6] also mentioned that an increased in the dimensionless ambient temperature and dimensionless figure of merit will increase the load resistance ratio but reduce the thermal conductance.

CHAPTER 3 RESEARCH METHODOLOGY

The simulations were conducted in three different part of simulation which were the combustion of the kerosene-vegetable cooking oil blend, the forced convection at the cold side of TEG with water cooled heat exchanger and the power generated by the TEG. Ansys fluid flow was used to simulate the combustion and forced convection while the power generated by TEG is simulated by Ansys Thermal-Electric. The output data from one stage is manually input into the next stage as input.

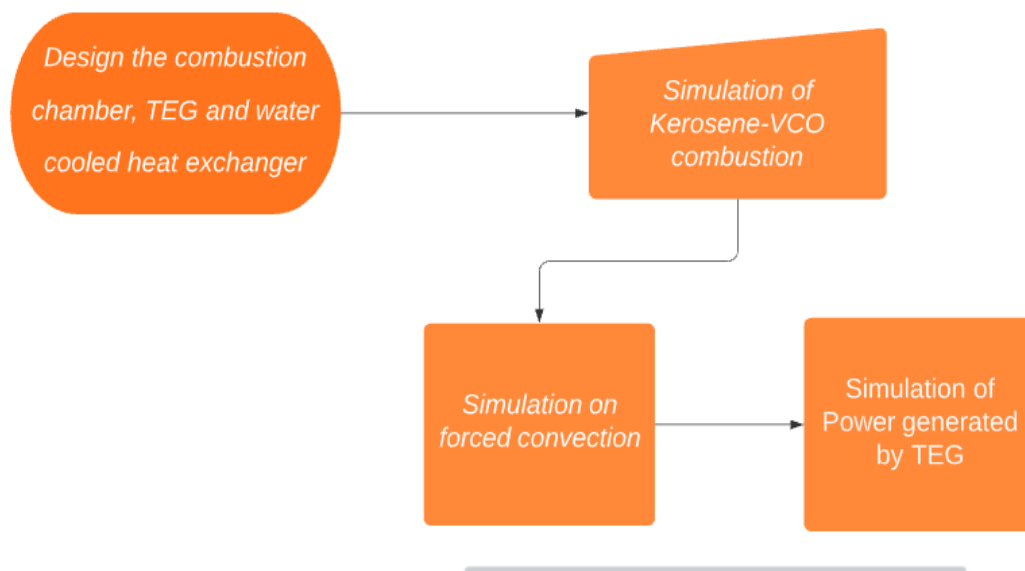


Figure 3-1 Summary of the simulation flow

3.1 Combustion modelling for hot side of TEG

The combustion modelling was performed in a chamber with a diameter of 150 mm and a height of 300 mm. Fuel blends of kerosene and vegetable cooking oil (VCO) were used to model the combustion process. Various fuel blends, mixture compositions, and equivalence air-fuel ratio, Φ were used to simulate the temperature of combustion as shown in [Table 3-1](#). This analysis was carried out to obtain the temperature profiles within the operating temperature of the TEG. Kerosene, $C_{12}H_{26}$ and VCO $C_{19}H_{38}O_2$ with a heating value of 43.1 MJ/kg and 39.66 MJ/kg, respectively were set in the simulation. In the simulation, the mass flow rate of fuel was set at constant value of 5×10^{-5} kg/s. From the simulation, the temperature within the operating temperature were selected.

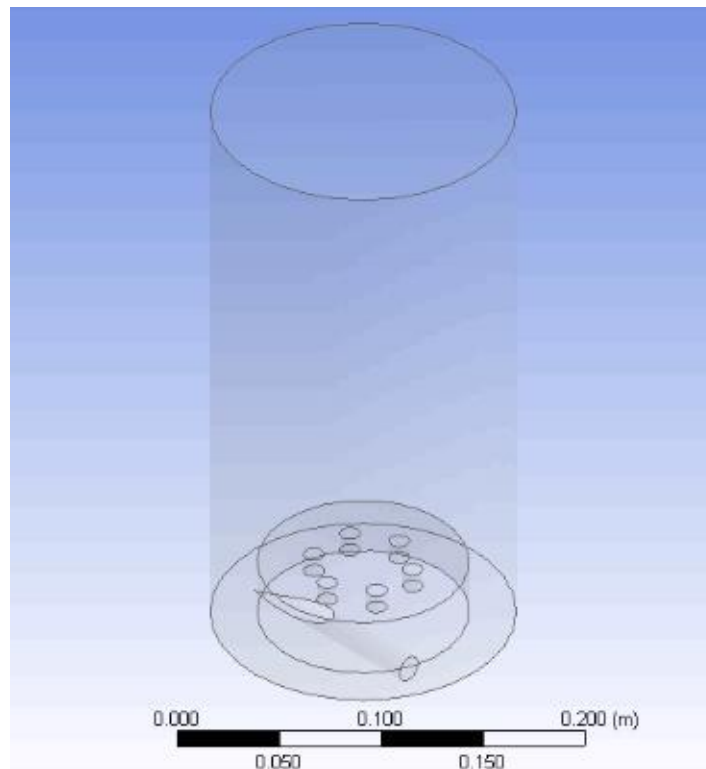


Figure 3-2 Combustion Chamber

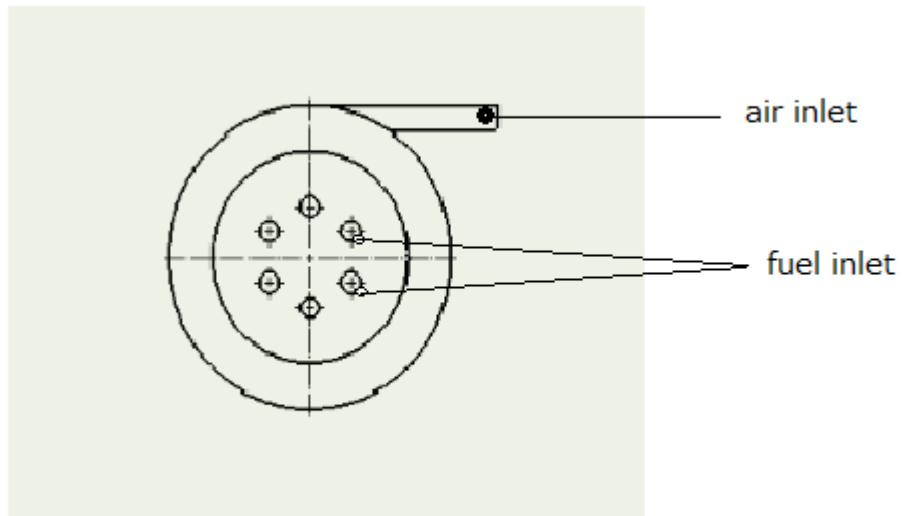


Figure 3-3 Bottom view of combustion chamber

Table 3-1 Mass flow rate of air and fuel

blend (%Kerosene)	Φ	Air Fuel Rate		Mass Flow Rate (kg/s)	
		Stoichiometric	Actual	fuel	air
100	0.1	14.9698	149.6976	5.00E-05	7.48E-03
	0.3	14.9698	49.8992	5.00E-05	2.49E-03
	0.75	14.9698	19.9597	5.00E-05	9.98E-04
	1	14.9698	14.9698	5.00E-05	7.48E-04
	1.25	14.9698	11.9758	5.00E-05	5.99E-04
90	0.1	14.7629	147.6290	5.00E-05	7.38E-03
	0.3	14.7629	49.2097	5.00E-05	2.46E-03
	0.75	14.7629	19.6839	5.00E-05	9.84E-04
	1	14.7629	14.7629	5.00E-05	7.38E-04
	1.25	14.7629	11.8103	5.00E-05	5.91E-04
75	0.1	14.4009	144.0090	5.00E-05	7.20E-03
	0.3	14.4009	48.0030	5.00E-05	2.40E-03
	0.75	14.4009	19.2012	5.00E-05	9.60E-04
	1	14.4009	14.4009	5.00E-05	7.20E-04
	1.25	14.4009	11.5207	5.00E-05	5.76E-04
50	0.1	13.8320	138.3203	5.00E-05	6.92E-03
	0.3	13.8320	46.1068	5.00E-05	2.31E-03
	0.75	13.8320	18.4427	5.00E-05	9.22E-04
	1	13.8320	13.8320	5.00E-05	6.92E-04

	1.25	13.8320	11.0656	5.00E-05	5.53E-04
25	0.1	13.2632	132.6316	5.00E-05	6.63E-03
	0.3	13.2632	44.2105	5.00E-05	2.21E-03
	0.75	13.2632	17.6842	5.00E-05	8.84E-04
	1	13.2632	13.2632	5.00E-05	6.63E-04
	1.25	13.2632	10.6105	5.00E-05	5.31E-04

3.2 The cold side of TEG

Once the temperature within the operating temperature was selected, the cold side temperature was simultaneously simulated. The cold side of the TEG was connected to a copper block and a water heat exchanger. The density, specific heat capacity and thermal conductivity of copper block is 8300 kg/m³, 385 J/kgK and 401 W/mK, respectively. Three water channels with 10mm diameter pass through the copper block. The flow rates of water were maintained at 0.005 kg/s, 0.01 kg/s and 0.03 kg/s for each channel used in the simulation.

Then, an equivalent values for the TEG were created to describe the thermal properties of TEG[15]. The equivalent thermal properties of TEG are,

The equivalent density,

$$\rho_{eq} = \frac{2m_1 + nm_1}{A_1 h_1} \quad 3.1$$

The equivalent thermal conductivity of TEG,

$$k_{eq} = \frac{1}{\frac{A_1}{nk_2 A_2} + \frac{2}{k_1}} \quad 3.2$$

The equivalent heat capacity of TEG,

$$C_{p\ eq} = \frac{1}{\frac{m}{nc_{p\ 1}m_2} + \frac{2m}{c_{p\ 1}m_1}}$$

3.3

Where m_1 is the mass of the ceramic composite, n is the number of n-type and p-type leg, A_1 is the area of the ceramic (40mm x 40mm), h_1 is the total height of the TEG (3.5 mm), A_2 is the area of the legs (1.4mm x 1.4 mm), k_1 is the ceramic thermal conductivity (31 W/mK), k_2 is the legs thermal conductivity (1.6 W/mK), m is the total mass, m_1 is the mass of the ceramic, m_2 is the mass of the legs, c_{p1} is the specific heat capacity of the ceramic (419 J/kgK) and c_{p2} is the specific heat capacity of the legs (200 J/kgK). From these values, an equivalent density, thermal conductivity and specific heat capacity of 2343.55 kg/m³, 0.4844 W/mK and 55.36 J/kgK were obtained.

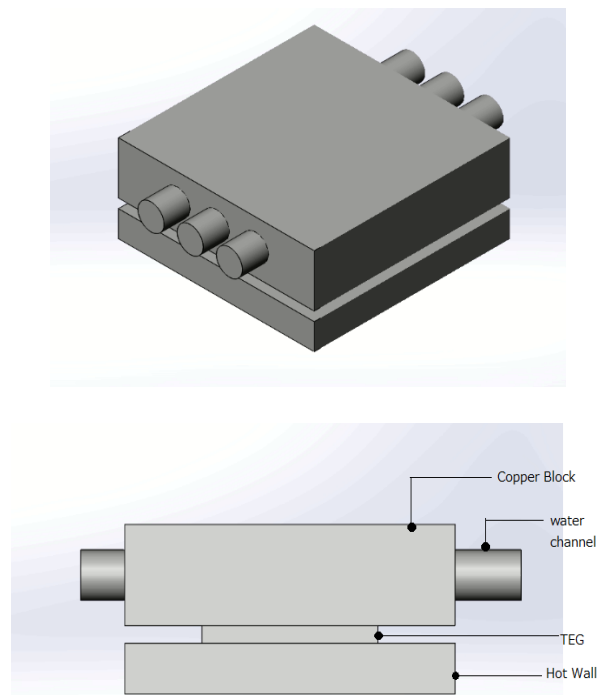


Figure 3-4 TEG with water heat exchanger

3.3 The power generated by TEG

The module consists of 256 thermoelectric legs that were connected in series with copper strip. The simulation was performed using the temperature distributions from the simulation in chapter 3.1 and chapter 3.2.

From the simulation, the voltage difference between the positive and negative sides and the current density was obtained. From the current density, the average current flow in the TEG was calculated by multiplying the average current density with the cross-sectional area of the copper strip (0.4 mm x 1.4 mm). Therefore, the power generated by the TEG was determined using the equation,

$$P= IV$$

Where, I is the current flow and V is potential difference of the negative and positive junction of the TEG.

CHAPTER 4 RESULTS AND DISCUSSION

4.1 Combustion modelling for hot side of TEG

Figure 4-1 shows the temperature distribution vertically along the wall of the combustion chamber. The plot shows that the temperature reduced as the height of the wall increased since the combustion started at the bottom of the combustion chamber. Meanwhile, Figure 4-2 shows the temperature distribution horizontally at two different heights of 0.075 m and 0.22 m. The temperature was low at the middle of the chamber.

The result from the simulation as in Figure 4-3 shows that the average temperature of the wall decreases when the percentage of kerosene content in the fuel blend was reduced. This is due to the higher LHV of kerosene compared with the VCO. Furthermore, an increased in the equivalence air fuel ratio, Φ caused a significant increase in the average temperature. At the rich mixture, the temperature is lower even with higher mass flow rate of fuel. This is due to the incomplete combustion of the fuel as a result of the insufficient air for combustion. Therefore, lower average temperature was obtained at lower value of Φ .

The highest average wall temperature of 1000K was recorded at 100% kerosene with Φ value of 1.25. However, this temperature was found to be unsuitable for the TEG application because the temperature is higher than the normal operating temperature of the TEG.

In order to validate this trend, another simulation was performed by maintaining the flow rate of the air but manipulating the mass flow rate of the fuel.

The results from Figure 4-4 show that the trend is almost similar to the preceding at constant mass flow rate of the fuel.

Previous studies on the combustion of kerosene and vegetable cooking oil blends by Mustafa et al. found that the maximum temperature with 100% kerosene at Φ value of 1 was found to be approximately 900°C [19]. The temperature values was used as a benchmark value to validate the simulation that was conducted in parallel.

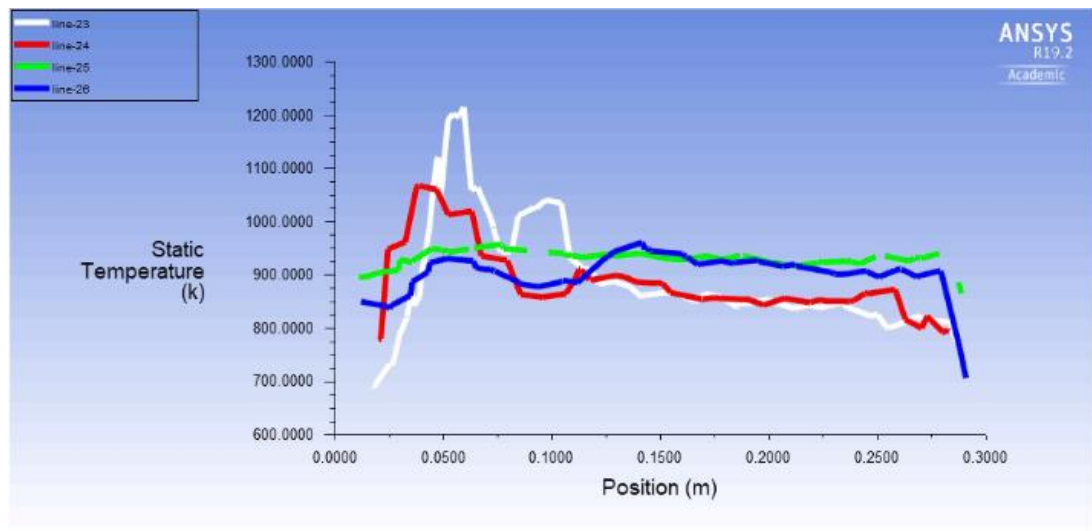


Figure 4-1 Temperature distribution of the wall

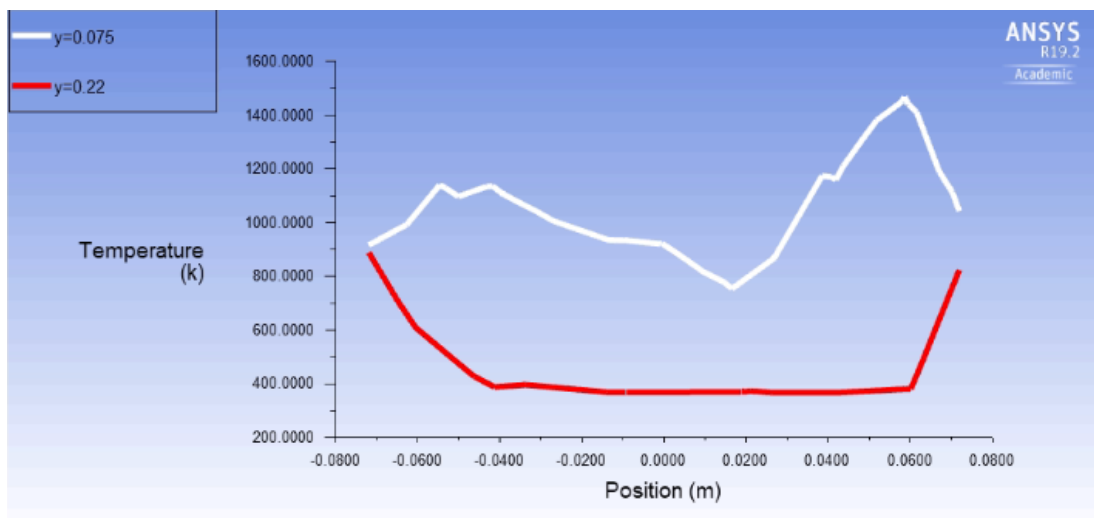


Figure 4-2 Temperature distribution along x-axis at y=0.075m and y=0.22m

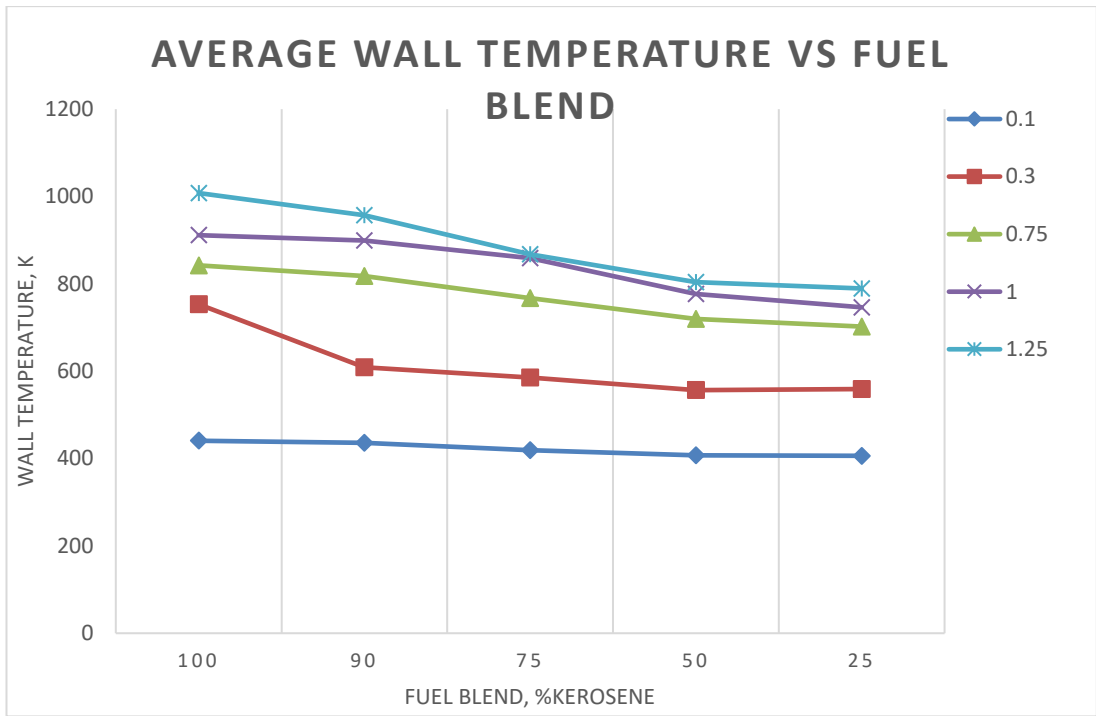


Figure 4-3 Wall Temperature Vs Fuel Blend at different Φ

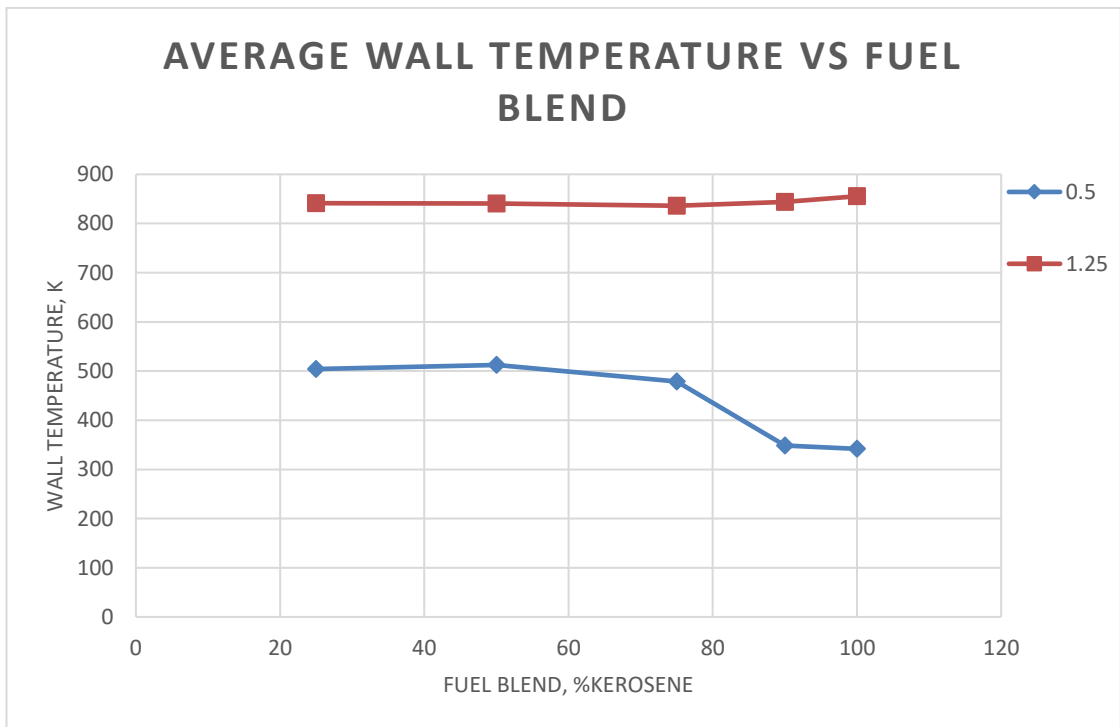


Figure 4-4 Wall Temperature Vs Fuel Blend at Different Φ with fix air flow rate

4.2 The cold side of TEG

From the simulation results, the wall temperature at Φ values of 0.30, 0.75 and 1.0 were chosen because these values are within the operating temperature of the TEG. The results show that the temperature difference between the hot and cold side of TEG increases with the increasing mass flow rate of the water. An increased in the temperature difference with an increased in the mass flow rate of the water was significantly low.

However, the temperature difference was markedly reduced by 50% when there was no water flow across the heat exchanger. From here we can conclude that the water flow assisted in reducing the temperature at the cold side of the TEG.

Figure 4-5 shows the contour plot of temperature distribution across TEG while Figure 4-6, Figure 4-7 and Figure 4-8 show the temperature different between the hot and cold side of TEG at different Φ value. From Figure 4-6 the highest temperature reduction of 493.7 K was observed at 100% kerosene at Φ value of 1.0 with the mass flow rate of water of 0.03 kg/s. With same fuel blend and Φ value, the temperature reduction was 487.9 K and 486 K when the mass flow rate of water was 0.01 kg/s and 0.005 kg/s, respectively.